AIR FORCE INSTITUTE OF TECHNOLOGY

AIR UNIVERSITY
UNITED STATES AIR FORCE

SCHOOL OF ENGINEERING

WRIGHT-PATTERSON AIR FORCE BASE, OHIO

AF-WP-O-MAY 62 3,500

INTERFEROMETER STUDY OF THE EFFECT OF REDUCED PRESSURE ON FREE CONVECTION FROM A VERTICAL PLATE

GAE/ME/62-5

Richard Clayton Walker
Capt USAF

AF-WP-O-SEP 62 25

INTERFEROMETER STUDY OF THE EFFECT OF REDUCED PRESSURE ON FREE CONVECTION FROM A VERTICAL PLATE

THESIS

Presented to the Faculty of the School of Engineering of
the Air Force Institute of Technology
Air University
in Partial Fulfillment of the
Requirements for the Degree of
Master of Science

By
Richard Clayton Walker, B.S.
Capt USAF

Graduate Aeronautical Engineering

August 1962

Preface

This report concerns an interferometer study of the effects of reduced pressure on free convection. The range of pressure investigated was from 0.98 atm to 0.09 atm.

During the study an accurate and inexpensive pressure regulator was developed which is described in the chapter on experimental apparatus. Also, a digital computer program for a table used to evaluate temperature from interferograms may be found in Appendix B. This program can be easily modified for any particular interferometer study.

I wish to express my appreciation to Dr. Andrew J. Shine, my faculty advisor, for his interest and valuable aid throughout the study. I also wish to acknowledge the assistance given me during the study by Frank Jarvis of the Mechanical Engineering Laboratory.

Richard C. Walker

Contents

Contents

List of Figures

List of Tables

List of Symbols

Symbol	Quantity	Unit
$\mathring{A}$	Wave length of light	Angstrom
C	Specific refractivity	ft^3/lb_m
g_c	Dimensional conversion constant	$ft\ lb_m/sec^2 lb_f$
Gr	Grashof number	
h	Heat transfer coefficient	$BTU/hr\ ft^{2o}F$
k	Thermal conductivity	$BTU/hr\ ft^{o}F$
L	Length	inches
Nu	Nusselt number	
P	Absolute pressure	atm
P_r	Prandtl number	
R	Gas constant	$ft^3/atm\ lb_m\ ^{o}R$
S	Scale factor of photograph	
T	Absolute temperature	^{o}R
dT/dy	Temperature gradient at the plate	$^{o}R/ft$
x	Distance along the plate	inches
Δy	Spacing between fringes at the plate as measured from photograph	inches
β	Coefficient of expansion	$1/^{o}R$
ε	Fringe number	
θ	$T_p - T_c$	^{o}F
λ_o	Wave length of light in vacuum	Angstrom

List of Symbols

Symbol	Quantity	Unit
μ	Dynamic viscosity	$lb_m/sec\ ft$
ρ	Density	$slugs/ft^3$
γ	Density	lb_m/ft^3
ϕ	Temperature difference between fringes at the plate	^oR

Subscripts

c	Chamber
p	Plate
r	Room conditions
x	Along the plate surface

Abstract

This report concerns an interferometer study of the effect of reduced pressure on free convection from a vertical plate. The interferometer was used to visually observe the boundary layer on the plate and to determine the heat transfer coefficient over a range of pressure from 0.987 atm to 0.09 atm. The free-convective heat transfer coefficient was experimentally found to be proportional to the 0.47 power of the pressure which is within experimental limits of the theoretical prediction (0.50 power of the pressure). The boundary layer thickness was observed to increase as the pressure was reduced.

GAE/ME/62-5

INTERFEROMETER STUDY OF THE EFFECT OF REDUCED PRESSURE ON FREE CONVECTION FROM A VERTICAL PLATE

I. Introduction

This is a report on an interferometer study of the effect of reduced pressure on free convection. The first chapter will include background information on the subject and the purpose, scope, and organization of the report.

Background Information

Past studies have been made of free convection at reduced pressures from spheres and horizontal cylinders. In 1924 Rice determined the free convection heat transfer from horizontal cylinders in air at pressures ranging from 0.11 atm to 1.0 atm (Ref 6:305). More recently (1954) Madden and Piret determined the free-convective heat transfer coefficient for spheres and wires in air, helium, and argon at pressures ranging form 5.0×10^{-6} atm to 1.0 atm (Ref 7:653).

In the studies conducted by Rice, Madden, and Piret, an indirect method was used to compute the free-convective heat transfer coefficient. First, they measured the total heat transfer coefficient, then subtracted from it a calculated value of the radiant heat transfer coefficient to obtain the free-convective heat transfer coefficient. Another method used to calculate the free-convective heat transfer coefficient makes use of the interferometer.

The interferometer makes it possible to compute the free-convective heat transfer coefficient directly. R. B. Kennard was the first to demonstrate this method when he published in 1931 the results of his experiments on free convection from a vertical plate. E. Eckert and E. Soehngen also used an interferometer to study free convection from a vertical plate in 1947. In their report they indicated a better agreement of heat transfer data existed between those who used the interferometer method than those who used the indirect method to calculate the free-convective heat transfer coefficient (Ref 4:8).

Purpose

Thus far free convection at reduced pressures has been experimentally investigated from cylinders and spheres using an indirect method to compute the heat transfer coefficient. The purpose of this study is to determine the effect of reduced pressure on free convection from a vertical plate by using the interferometer as a means to measure the free-convective heat transfer coefficient directly, and to observe the boundary layer. This study is unique in that the interferometer is used to study free convection at sub-atmospheric pressures.

Scope

This study considers only laminar free convection at air pressures ranging from 0.09 atm to .987 atm on a verti-

cal surface with uniform temperature distribution. The temperature of the plate is varied from 170°F to 230°F.

Organization

The remainder of the report will be divided into the following sections: (1) problem analysis, (2) apparatus, (3) experimental procedures, (4) evaluation of data, (5) results, (6) discussion of results, and (7) conclusions.

II. Problem Analysis

In this chapter the problem of determining the effect of pressure on free convection is analysed. This is done to find what quantities must be determined experimentally in order to obtain a solution to the problem.

This chapter will be presented in three parts: (1) dimensionless parameters used in the solution to the problem, (2) solution to the problem and (3) assumptions necessary to solve the problem.

Dimensionless Parameters

In the determination of the free-convective heat transfer coefficient it is convenient to use dimensionless parameters.

The dimensionless parameters used in the study of free convection are the Nusselt, Grashof, and Prandtl numbers. The application of dimensional analysis to free convection produces the dimensionless parameters and the relationship among the parameters as shown in Eq (1)

$$Nu = C(Gr\,Pr)^m \tag{1}$$

where C and m are constants (Ref 5:69,75). To find the value of the constants C and m ; the Nusselt, Grashof, and Prandtl numbers must be determined.

Nusselt Number. The Nusselt number can be determined experimentally by equating the heat flow through the boundary layer as defined by h [left side of Eq (2)] to the expression for the heat conduction through the stagnant film of air on the surface of the plate [right side of Eq (2)].

$$h\theta = k\left[\frac{dT}{dy}\right] \tag{2}$$

Multiplying Eq (2) by x and solving for the expression $\frac{hx}{k}$, which is the Nusselt number based on the length x, gives

$$Nu_x = \frac{hx}{k} = \left[\frac{dT}{dy}\right]\frac{x}{\theta} \tag{3}$$

The temperature gradient can be determined from interferograms and the quantity θ by measurements of the plate and ambient temperatures. Thus the Nusselt number can be experimentally determined at any point x along the plate by use of Eq (3).

Grashof Number. The Grashof number represents the ratio of buoyant forces to the viscous forces and is given by

$$Gr_x = \frac{\rho^2 g_c \beta \theta x^3}{\mu^2} \tag{4}$$

If the perfect gas equation of state is used to eliminate ρ, Eq (4) becomes

$$Gr_x = \frac{g_c p^2 \beta \theta x^3}{R^2 T^2 \mu^2} \tag{5}$$

which is the Grashof number based on x now expressed as a known function of pressure. The quantities appearing in Eq (5) are either known or can be determined experimentally; therefore, the Grashof number can be determined at any point x along the plate.

Prandtl Number. The Prandtl number is given by Eq (6) and can be found directly from the air tables.

$$Pr = \frac{c_p \mu}{k} \tag{6}$$

Solution

With the values of Nu, Pr, and Gr known, the constants C and m appearing in Eq (1) can be determined. Eq (1) may be written as

$$Nu_x = \frac{hx}{k} = C\left[\frac{g_c C_p P^2 \beta \theta x^3}{R^2 T^2 \mu k}\right]^m \tag{7}$$

from which the effect of pressure on the heat transfer coefficient can be seen to be

$$h \propto p^{2m} \tag{8}$$

where m can be experimentally determined.

Assumptions

Some of the important assumptions used to obtain the relation in (8) will be discussed in this section. They include assumptions concerning a perfect gas, inertia forces, continuum, and free-molecule conduction.

Perfect Gas. The assumption that air behaves as a perfect gas was used to obtain the Grashof number as a function of pressure as shown in Eq (5). The air considered in this study is far below the critical pressure of air; therefore, the perfect gas assumption is valid (Ref 9:41).

Inertia Forces. The inertia forces of the fluid in the boundary layer are neglected in the relationship between the Nusselt, Grashof, and Prandtl numbers as expressed in Eq (1). For air this is a good assumption (Ref 3:316).

Continuum. In this study it is assumed that the air can be treated as a continuum, even though the pressure of the air is as low as 0.09 atm. In the concept of a continuum, the macroscopic properties describing the gross behavior of the substance is dealt with instead of dealing with the instantaneous state of many molecules. The concept of the continuum is valid as long as the mean free path of the molecules is not of comparable size with the smallest dimension of the plate (Ref 9:4). The mean free path of air molecules at 0.09 atm and 80°F is 3.48×10^{-4} inches.

Free-Molecule Conduction. According to Blodgett and Langmuir, heat is lost by free-molecule conduction from the

solid through the gas for a distance equal to the mean free path of the gas molecules (Ref 7:653). In this study the resistance to free-molecule heat conduction is neglected. In other words, the temperature of the film of air next to the plate is assumed to be at the temperature of the plate. Free convection experiments by Madden and Piret with spheres and wires at low pressures revealed that the resistance to free-molecule conduction can be neglected as long as the air can be treated as a continuum (Ref 7:653).

III. Experimental Apparatus

In this chapter a description of the experimental apparatus used in the study is presented. The experimental apparatus, as shown in Fig. 1, can be divided into three main components: (1) interferometer, (2) test plate, and (3) vacuum system.

Interferometer

The interferometer consists of an optical arrangement, a light source, and a camera.

Optical Arrangement. The interferometer used in this study has the Zender-Mach type optical arrangement with eight inch diameter optical parts. Complete information on the arrangement of the optical system may be found in (Ref 4:4).

Light Source. The light source of the interferometer consists of a lamp and filter. Fig. 2 shows the spectrum, wavelength, and relative intensity of the light emitted from the mercury lamp used in this study. A Wratten 77A filter was used in combination with the mercury lamp to produce 5461Å monochromatic green light.

A Cenco monochromatic filter which passes 4358Å light from the mercury spectrum was also used to produce a blue light.

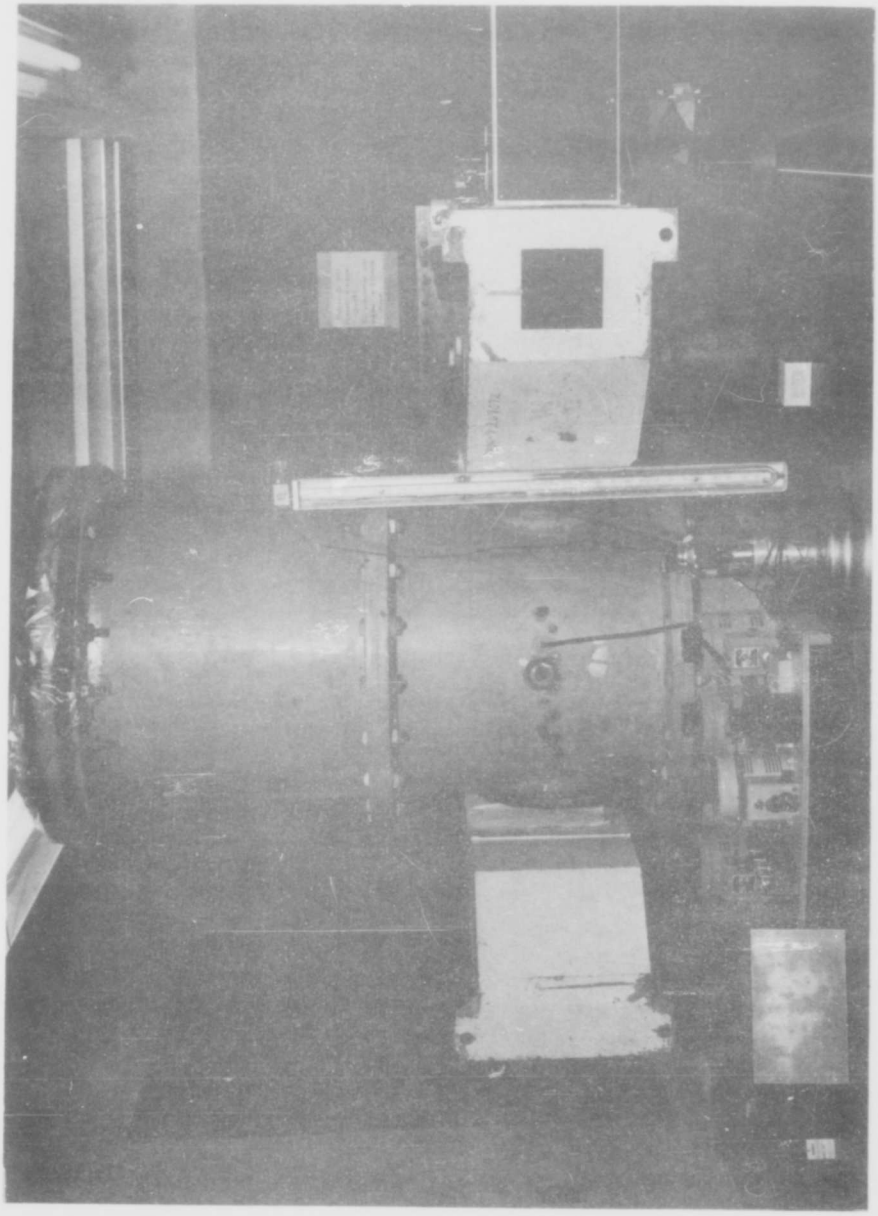

Fig. 1
Experimental Apparatus

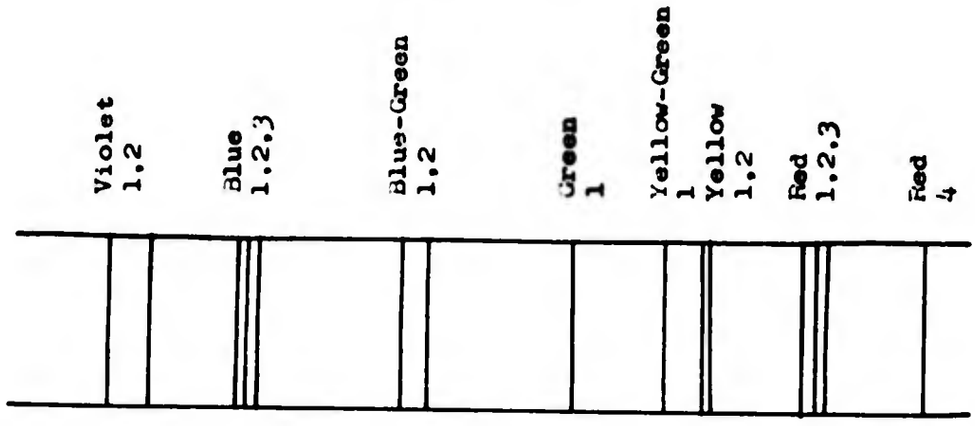

Mercury Spectrum

Line	Wavelength Å	Relative Intensity
Violet 1	4047	10
Violet 2	4173	7
Blue 1	4339	6
Blue 2	4348	6
Blue 3	4358	10
Blue Green 1	4916	5
Blue Green 2	4960	5
Green 1	5460	10
Yellow Green 1	5676	5
Yellow 1	5720	10
Yellow 2	5791	10
Red 1	6073	5
Red 2	6123	6
Red 3	6234	6
Red 4	6908	10

Fig. 2

Mercury Light Spectrum

(From Ref 8:95)

Camera. A 3 X 5 Graflex camera with a Polaroid back was used to obtain the interferograms. Type 42 Polaroid film was used with the green light and type 47 film was used with the blue light.

Test Plate Components

The components of the test plate were a plate, a power control unit, and a thermocouple system.

Plate. The plate, made from cast aluminum, is six inches high and ten inches long. Four individual heaters were used to heat the plate to temperatures as high as 300°F. Four iron-constantan thermocouple junctions were inserted from the rear of the plate and held close to the surface by countersunk screws. The face of the plate was made smooth by sanding the aluminum cement which was used to cover the screw heads.

Power Control Unit. The power control unit consisted of one master voltage regulator and four powerstat type voltage regulators. Each of the four regulators was connected directly to a corresponding heating element.

Thermocouples. The four iron-constantan thermocouples from the plate were connected to a Rubicon potentiometer by means of a selector switch. An ice-water mixture was used as the reference temperature in determing the plate temperature.

Vacuum System

The vacuum system was used to produce and maintain pressures from 0.09 atm to 1.0 atm. The main components of the vacuum system are the chamber, the pump, and the automatic pressure regulator.

Chamber. The chamber is seven feet high and two and one half feet in diameter. It is made of metal except for the top cover which is wooden, and the two 8-inch diameter interferometer windows. A thermometer was inserted into the chamber to register the chamber air temperature.

Pump. A Cenco-Hypervac 25 vacuum pump was used to evacuate the air from the chamber.

Pressure Regulator. Fig. 3 shows a pressure regulator which was developed during the course of the study. The components of the pressure regulator are a mercury manometer, two wire contacts, and a solenoid valve.

The mercury manometer served two purposes in the operation of the regulator. First, the manometer indicated the pressure in the chamber; and second, the mercury served as a conductor between the two wire contacts inserted in the manometer tube.

The desired pressure was set by vertical positioning of the wire contacts in the manometer tube. The wire contacts completed a circuit to the solenoid valve which regulated the amount of air leaving the chamber. The pressure in the chamber was controlled by the regulator to within $\pm$ 0.01 inches of mercury.

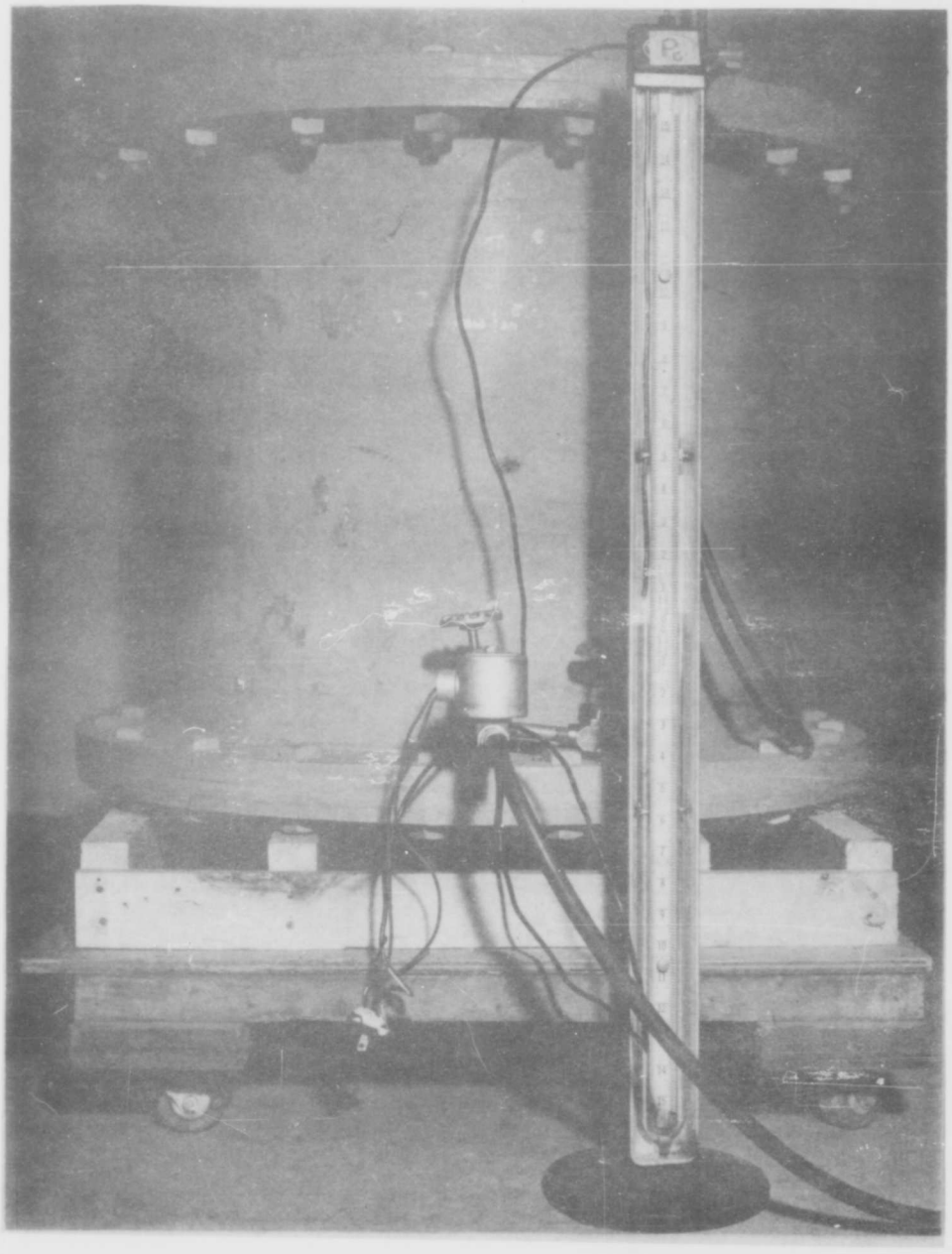

Fig. 3

Pressure Regulator

IV. Experimental Procedure

In this chapter the procedures used to obtain the data necessary to compute the Nusselt, Grashof, and Prandtl numbers are presented. The discussion of experimental procedures can be divided into two areas: (1) the preliminary procedures and (2) the obtaining of data.

Preliminary Procedure

The preliminary procedures concerned mainly the test plate and the interferometer.

Test Plate. The test plate was placed in the vacuum chamber and aligned with the interferometer by visual means. The vertical alignment of the plate was checked by comparing a plumb bob with the edge of the vertical portion of the shadow cast by the plate.

A uniform plate temperature to within $\pm$ 2°F was obtained by adjusting the power input to the four plate heaters.

Interferometer. Instructions in (Ref 2:12) were used as a guide to adjust the interferometer to produce fringes. All interferograms used as test data were taken with the interferometer adjusted to the infinite-fringe (Fig. 4a), as opposed to the finite-fringe adjustment (Fig. 4b). The fringes in Fig. 4a represent lines of constant temperature since the pressure is assumed to be constant in the boundary layer.

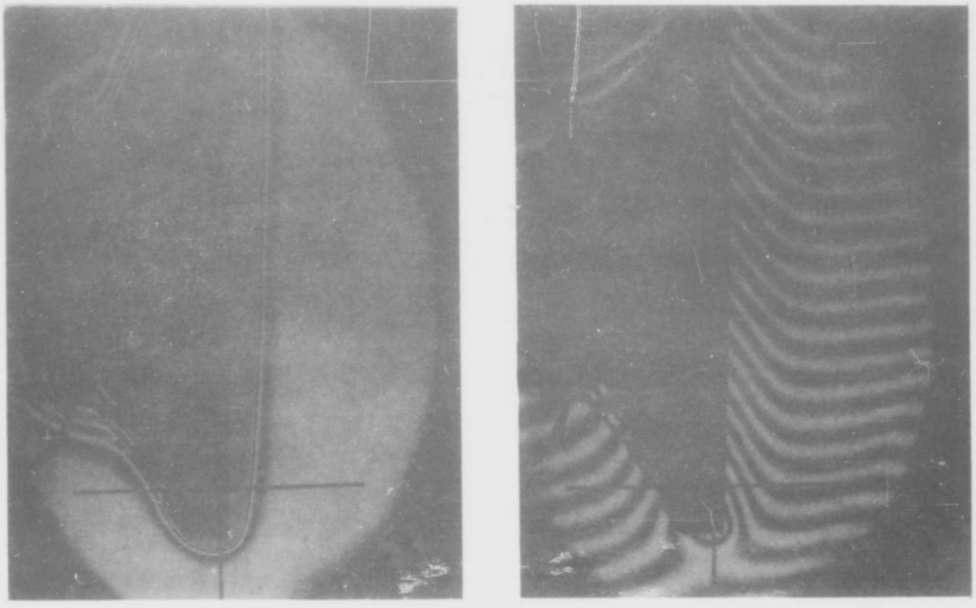

(a) infinite fringe (b) finite fringe

Fig. 4

Interferograms

Obtaining Data

The data was obtained in the following manner:

1. The desired vacuum in the chamber was set and maintained by the pressure regulator.

2. The plate temperature was allowed to stabilize which required about one hour for a chamber pressure change of one inch of Hg. The temperature was considered stabilized when the plate temperature remained constant for approximately ten minutes.

3. Two interferogram photographs were taken at the stabilized plate temperature. The photographs were marked to indicate the wavelength of light which exposed the film.

4. At the time the photographs were taken the chamber temperature, chamber pressure, plate temperature, room temperature, and barometric pressure were recorded.

5. The regulator was set to a new chamber pressure and procedures 2 through 5 were repeated until the desired amount of data was obtained.

Two sets of data were taken in an effort to check on the reproducibility of results. Table I in Appendix A shows the first set of data that was obtained with a plate-chamber temperature difference of 101°F at ambient pressure. The second set of data shown in Table II, Appendix A was obtained with an initial plate-chamber temperature difference of 86°F.

V. Evaluation of Data

The data were reduced to two dimensionless quantities: the Nusselt number, and the product of the Grashof and Prandtl numbers. However, before the data could be reduced to Nusselt numbers, the temperature gradient of the air near the plate had to be evaluated from the interferograms. In this chapter the evaluation of the interferogram, the Nusselt number, and the product of the Grashof and Prandtl numbers are discussed.

Interferograms

All interferograms were evaluated at stations two, three, and four inches from the leading edge of the plate to determine the temperature gradient at the plate. The method used to evaluate the temperature gradient follows a method used by Shine. This method consisted of dividing the temperature difference between fringes near the heated surface, by the spacing between the same fringes. Shine found that the above method agreed very well with the longer temperature-profile method which is often used to find the temperature gradient (Ref 10:60).

Spacing between Fringes. The spacing between fringes was measured by using a Gaertner comparator. The photograph was aligned with the vertical hairline of the microscope

coincident with the edge of the plate and the horizontal hairline on the station of the plate to be evaluated. The distance Δy was measured from the center of the second black fringe to the center of the first black fringe as counted from the plate. Since Δy was measured on photographs which were not of actual size, a scale factor (S) had to be determined.

The scale factor was determined by dividing the measured length of the reference wire from the photograph, by three inches, the known length of the reference wire. The scale factor for most of the photographs was 0.604. Considering the scale factor and the conversion of inches to feet, the spacing between the two fringes nearest the wall is given by $\frac{\Delta y}{S l 2}$.

Temperature Difference between Fringes. The difference between the temperature of any fringe ϵ and the chamber temperature is given by Eq (9)

$$\Delta T = T_c \left[\frac{\lambda_o \epsilon}{CL\gamma_c - \lambda_o \epsilon} \right] \qquad (9)$$

where ϵ is counted from the undisturbed air toward the plate.

In this study Eq (9) was used to calculate the temperature of the two fringes nearest the plate. The temperature difference between the two fringes was called ϕ. Table III in Appendix B was prepared using a digital computer from the bracketed portion of Eq (9). When the value of γ_c and ϵ are known, the table gives the value of the brac-

keted portion of Eq (9) which facilitates the use of the equations. The development of Eq (9) and the computer program for Table III are given in Appendix B.

Temperature Gradient. The expression for the temperature gradient at the plate in terms of the quantities just discussed becomes

$$\frac{dT}{dy} = \frac{S12\phi}{\Delta y} \tag{10}$$

Nusselt Number

The Nusselt number was found by combining Eq (3) and Eq (10)

$$Nu = \frac{Si2\phi x}{\Delta y \theta} \tag{11}$$

Product of Grashof and Prandtl Numbers

The product of the Grashof and Prandtl numbers was found by combining Eq (4) and Eq (6)

$$PrGr_x = \left(\frac{c_p \rho^2 \beta \theta x^3 g_c}{k \mu} \right) \tag{12}$$

or

$$PrGr_x = q \theta x^3 \tag{13}$$

where

$$Q = \frac{g_c \rho^2 \beta c_p}{k \mu} \qquad (14)$$

The value of Q for air at standard atmospheric pressure is shown as a function of temperature in Fig. 5. For other pressures Q must be multiplied by the square of the pressure in atmospheres (Ref 1:167). The values of Q used in the quantity $P_r G_r$ were obtained using the mean value of the plate and chamber temperatures.

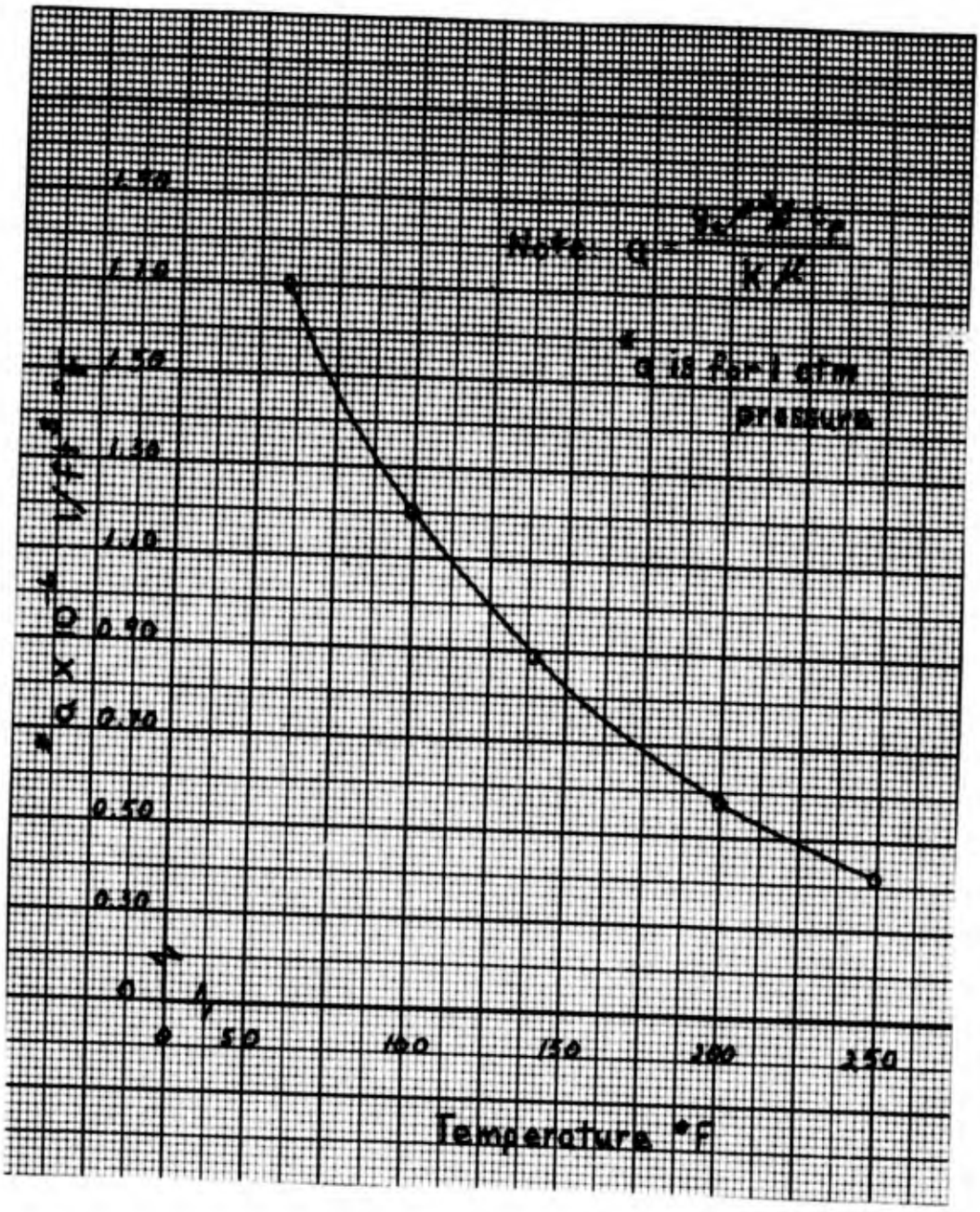

Fig. 5

Air Properties in (PrGr) vs. Temperature

(From Ref 1:306)

VI. Results

The results of this study will be given in two parts: (1) the effect of reduced pressure on the heat transfer coefficient, and (2) the effect of reduced pressure on the boundary layer.

Effect of Reduced Pressure on the Heat Transfer Coefficient

Figs. 6, 7, and 8 show the effect of reduced pressure on free convection at stations two, three, and four inches from the leading edge of the plate. In Chapter II it was shown that

$$h \propto p^{2m} \tag{8}$$

The slope of the line faired through the experimental points on each of the Figs. is the value of m. The average value of m from Figs. 6, 7, and 8 was found to be 0.235. Therefore

$$h \propto p^{.470}$$

In other words, the heat transfer coefficient is approximately proportional to the square root of the pressure.

Fig. 9 is a combined plot of the points in Figs. 6, 7, and 8 to show the variation of Nusselt number with pressure and with distance from the leading edge of the plate.

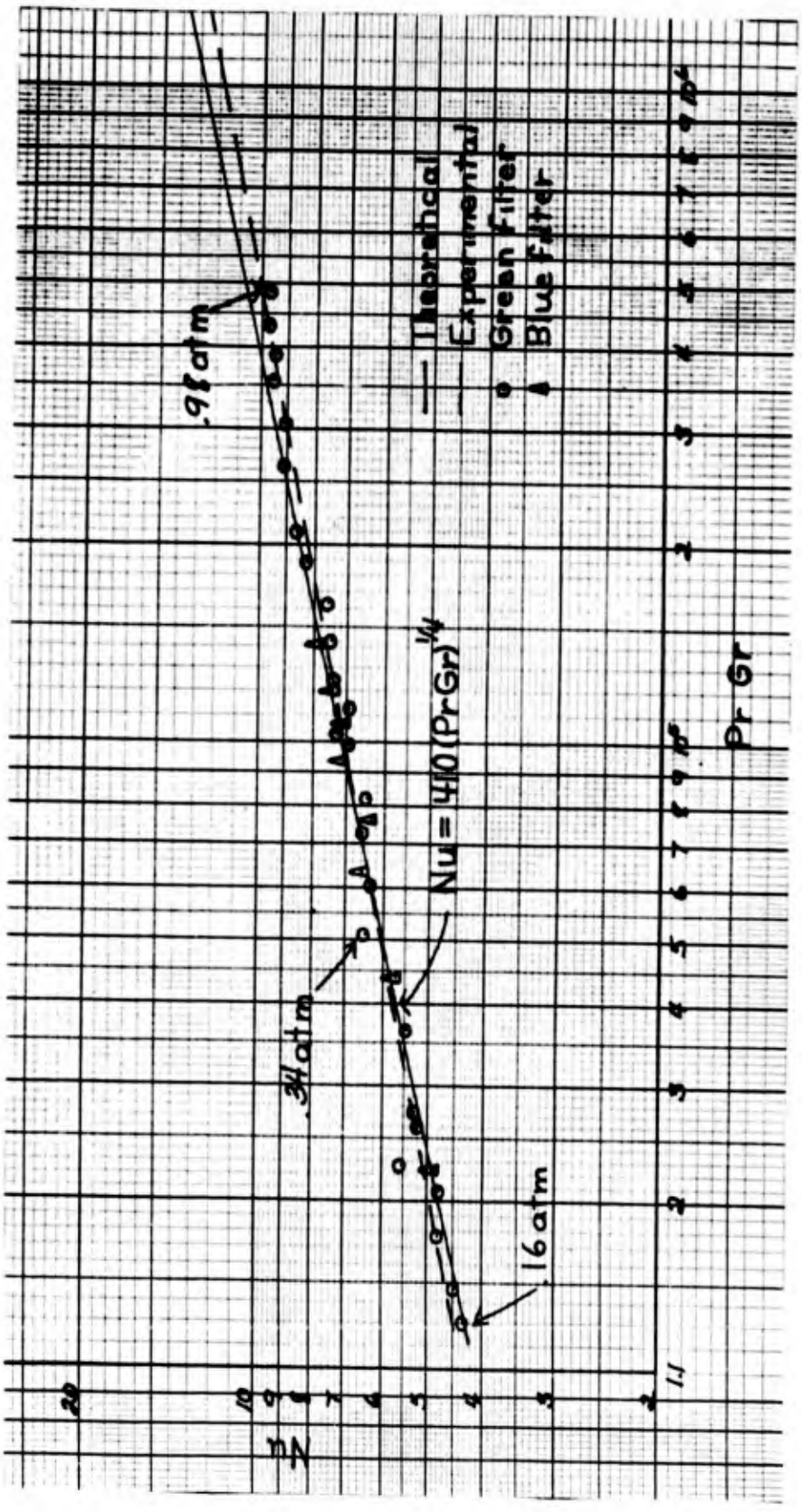

Fig. 6

Nu vs. PrGr at Station x = 2 Showing the Effect of Pressure on Free Convection

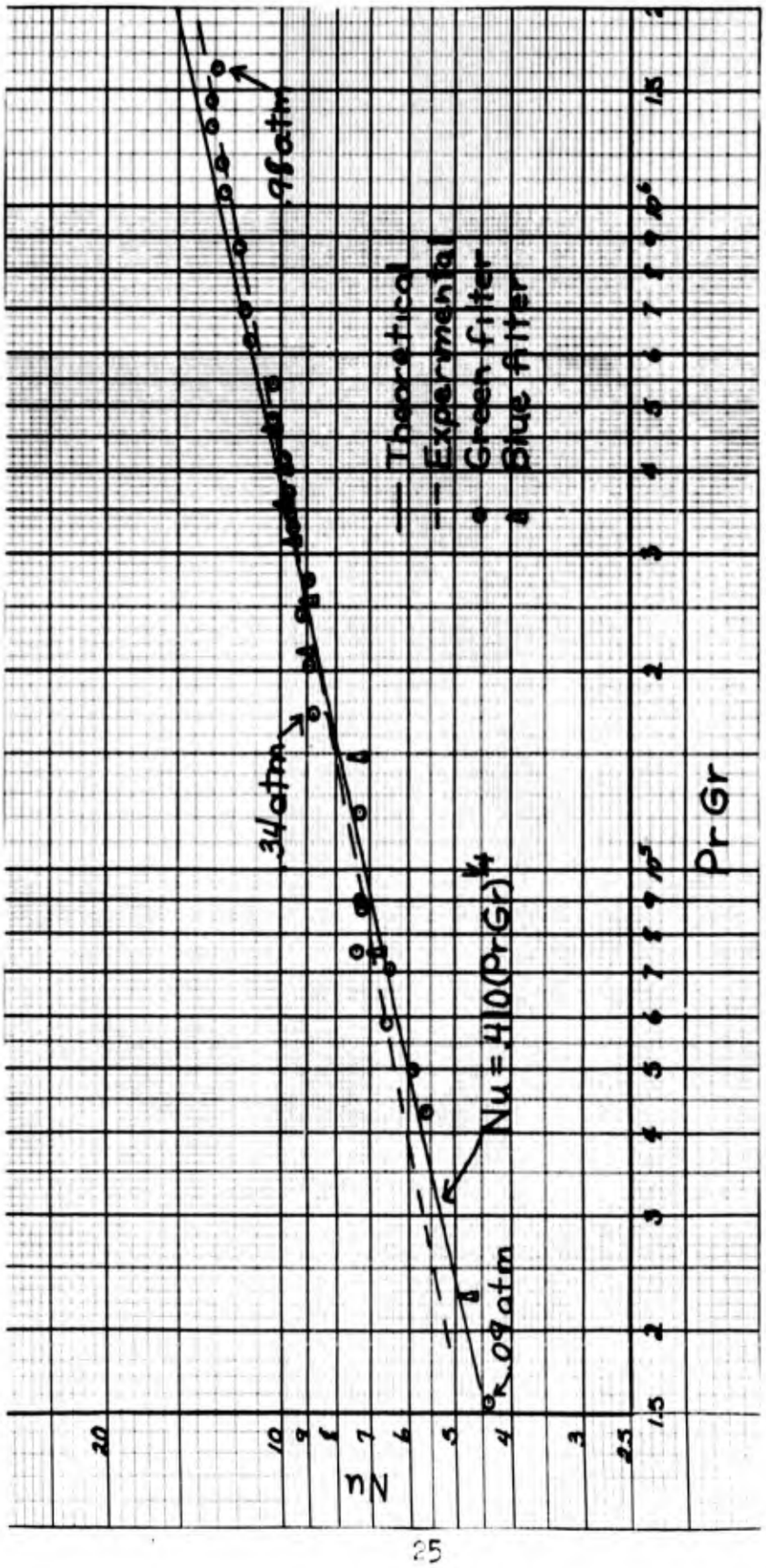

Fig. 7

Nu vs. PrGr at Station x = 2 Showing the Effect of Pressure on Free Convection

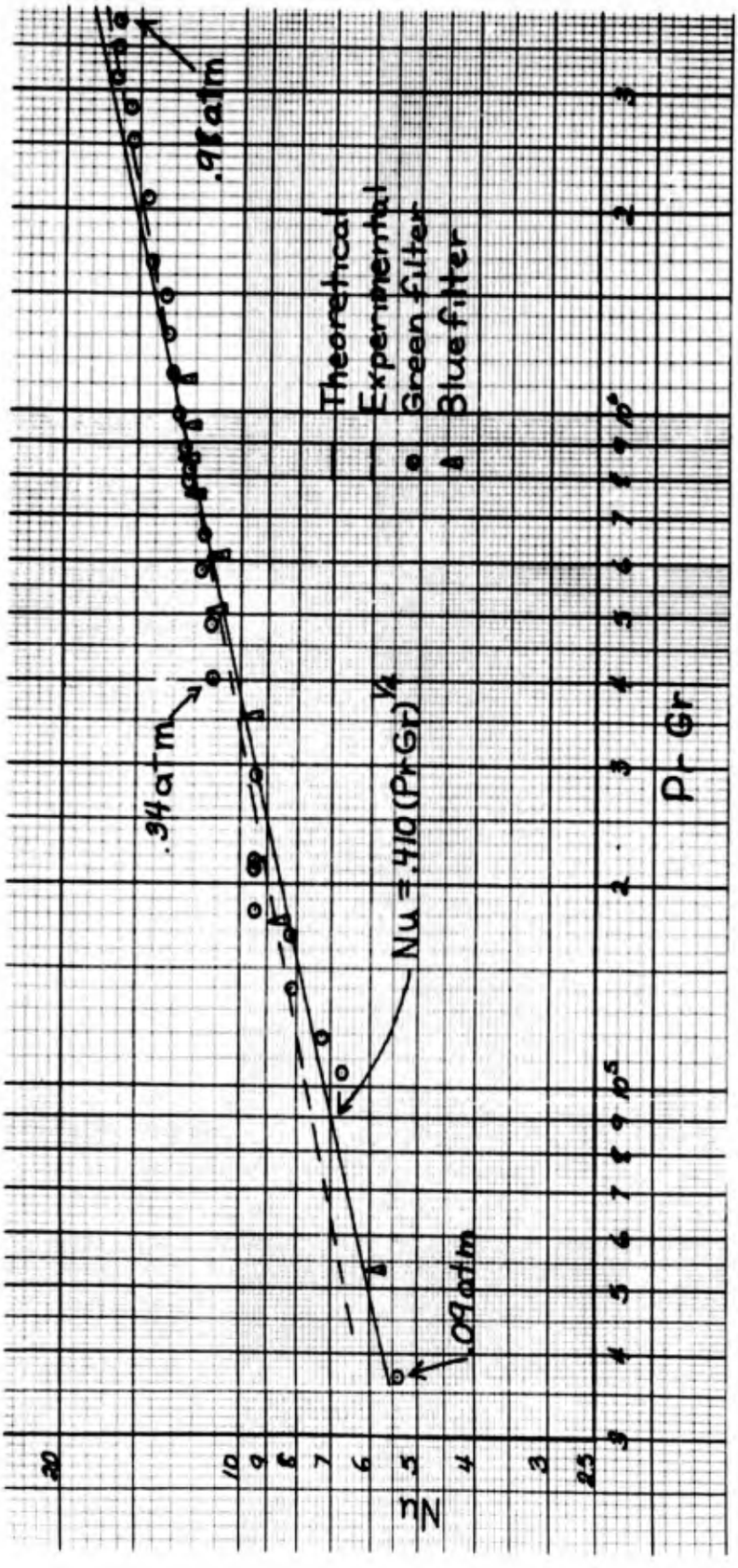

Fig. 8

Nu vs. PrGr at Station x = 4 Showing the Effect of Pressure on Free Convection

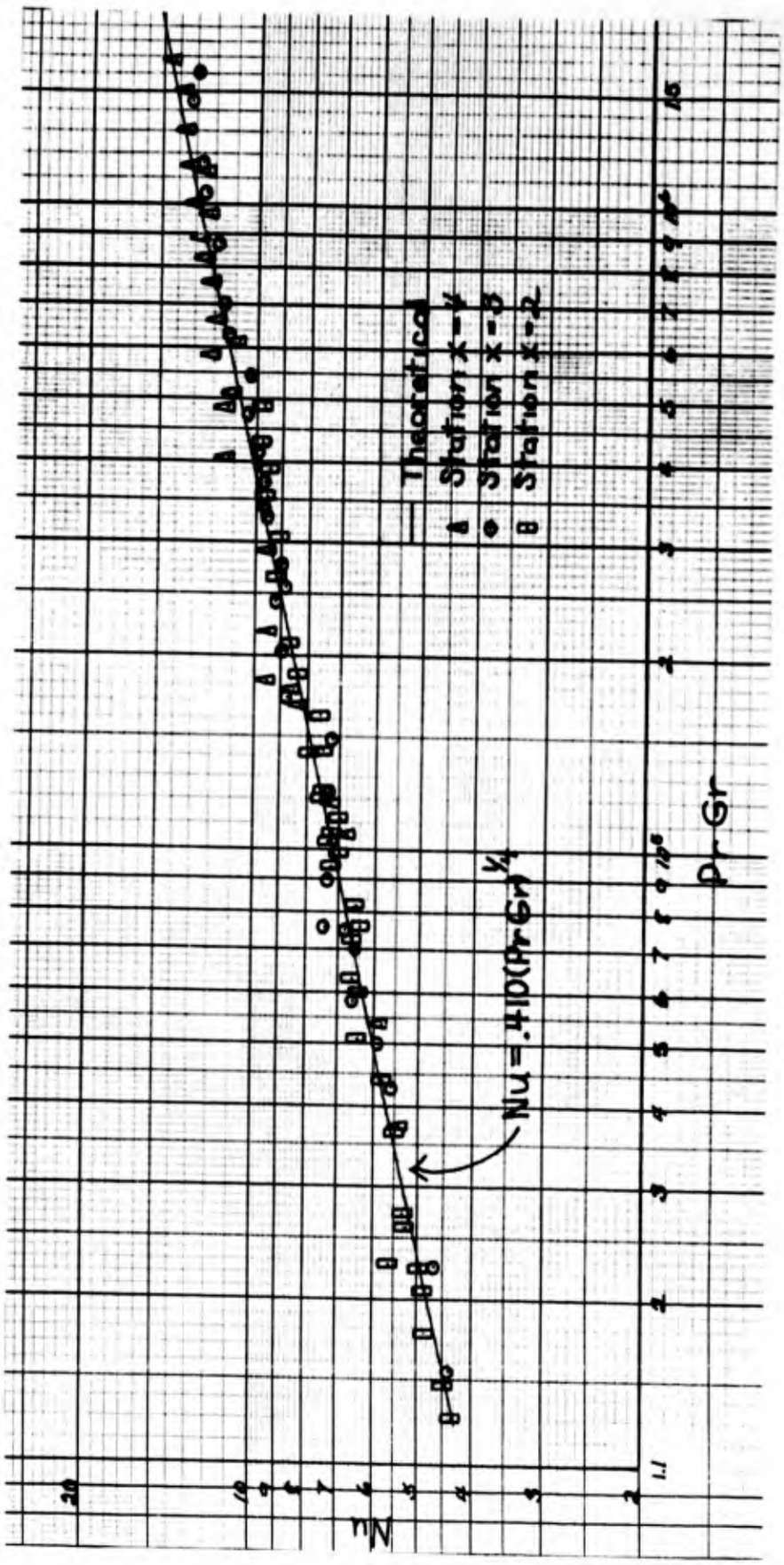

Fig. 9

Nu vs. Pr Gr at Station x = 2, 3, and 4 Showing the Effect of Pressure and x on Free Convection

Effect of Reduced Pressure on the Boundary Layer

The boundary layer was observed to become thicker as the pressure was decreased. Figs. 10, 11, 12, 13, and 14 show the actual size of the plate and boundary layer at various chamber pressures.

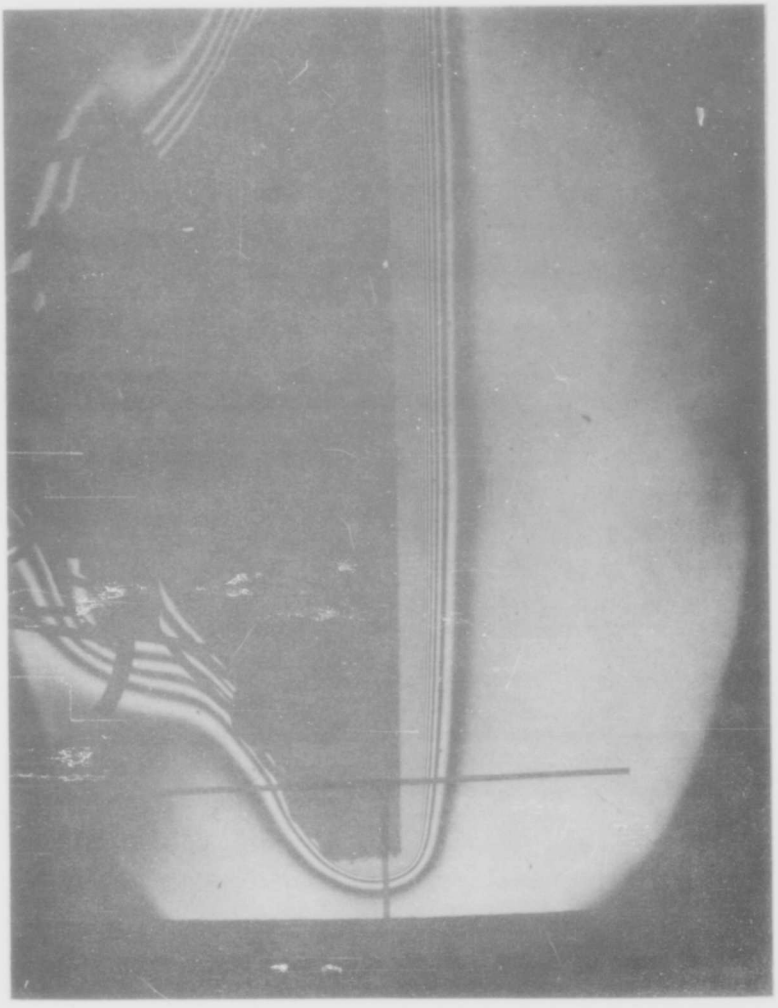

$\theta = 89.8^{\circ}F$ $T_{\rho} = 160^{\circ}F$

Fig. 10

Actual Size Interferogram of Boundary Layer on a Vertical Plate at 0.955 atm Pressure

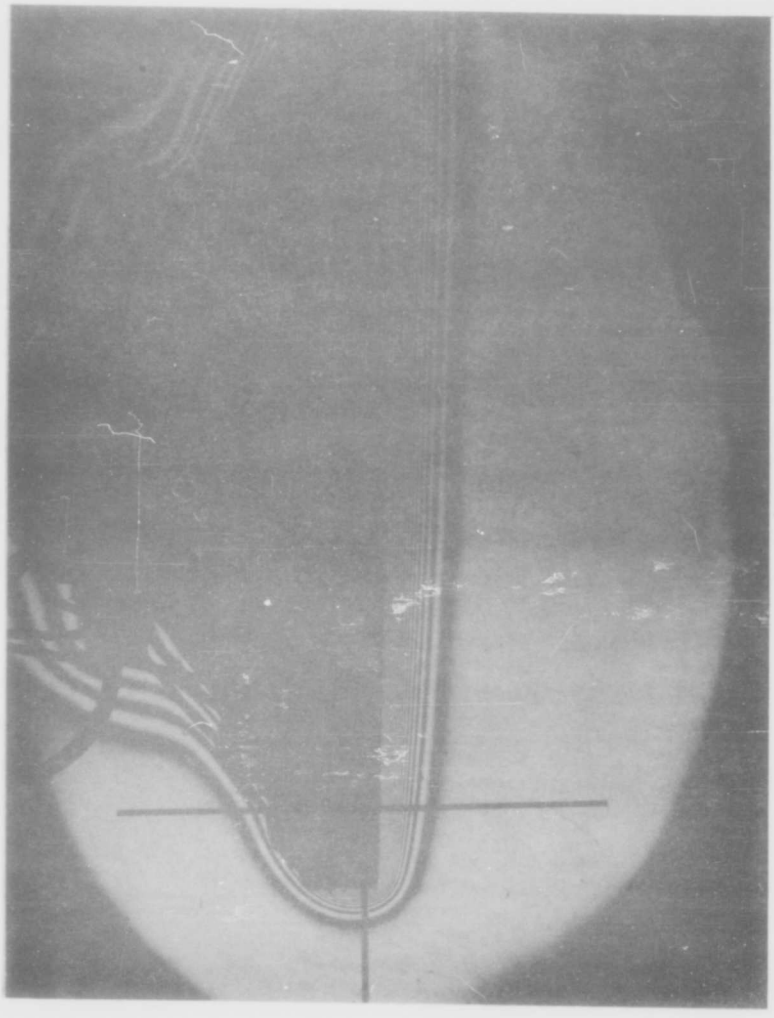

θ = 94.1°F T_p = 170.2°F

Fig. 11

Actual Size Interferogram of Boundary Layer on a Vertical Plate at 0.785 atm Pressure

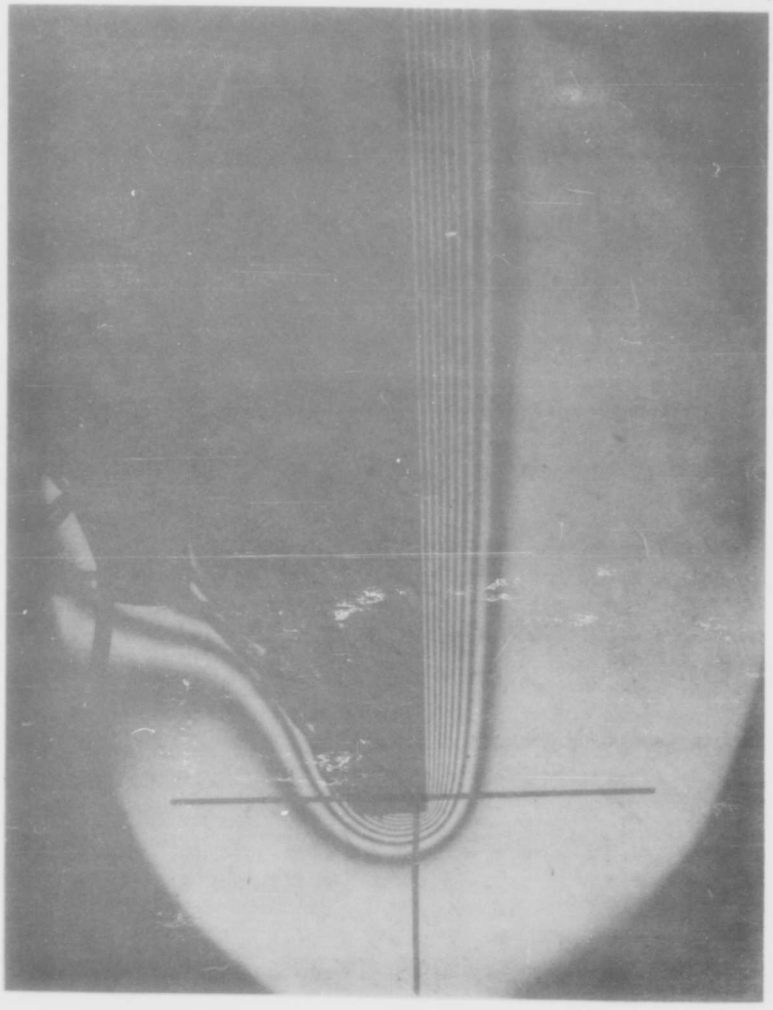

θ = 127.2°F T_p = 205.0°F

Fig. 12

Actual Size Interferogram of Boundary Layer on a Vertical Plate at 0.342 atm Pressure

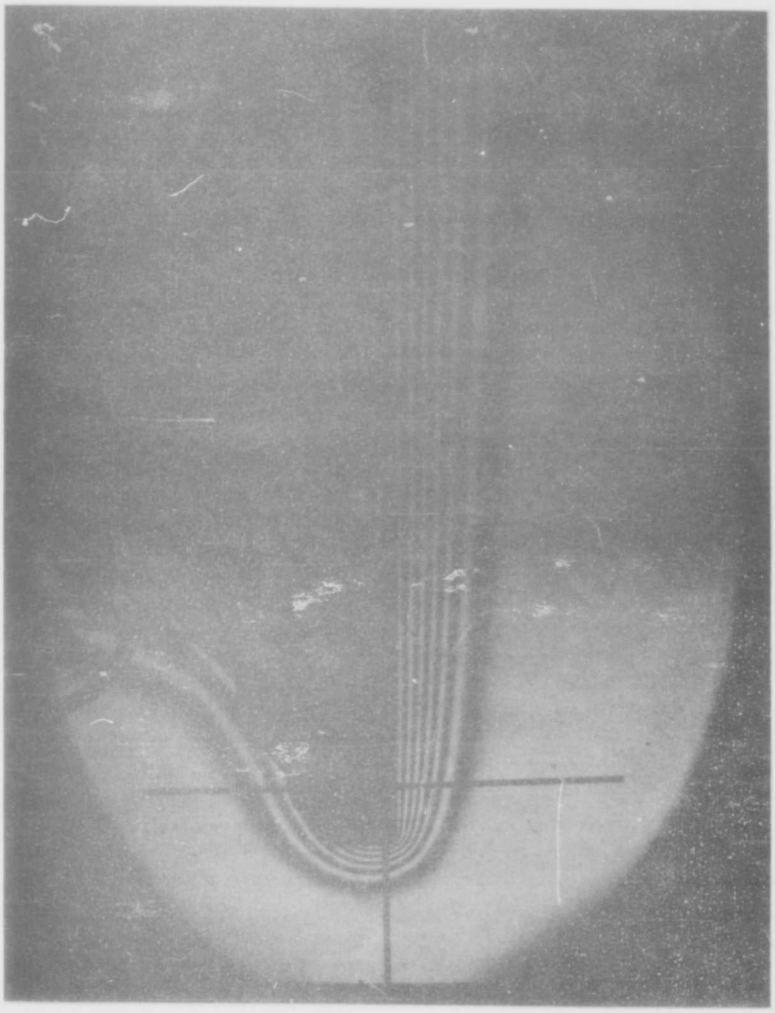

θ = 150°F T_p = 226°F

Fig. 13

Actual Size Interferogram of Boundary Layer on a Vertical Plate at 0.210 atm Pressure

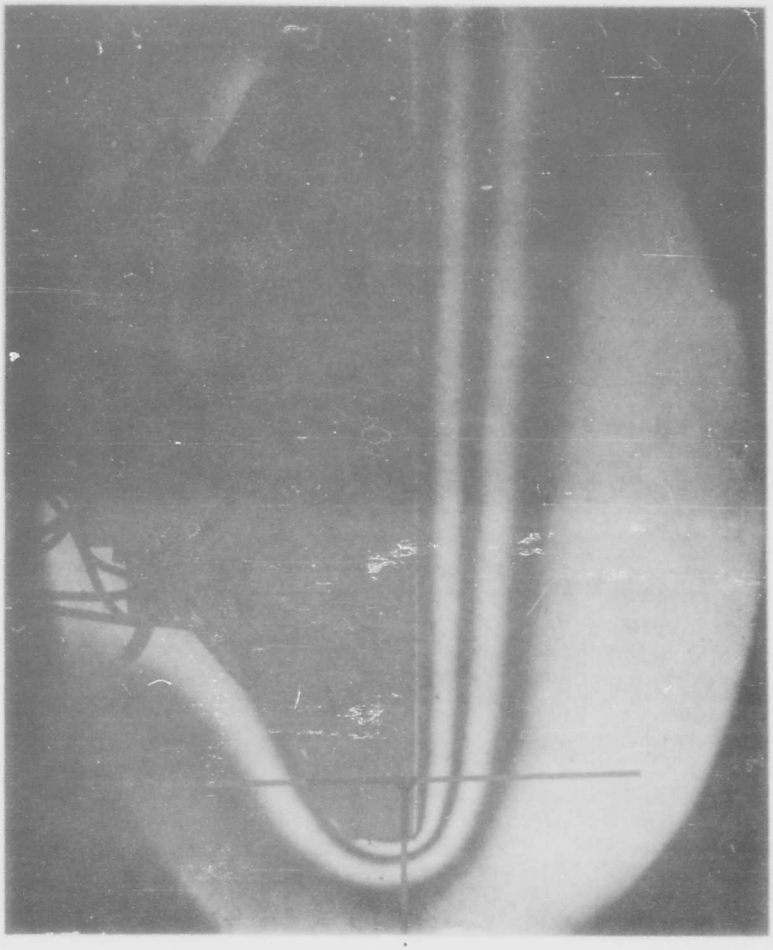

θ = 149.0°F T_p = 228.0°F

Fig. 14

Actual Size Interferogram of Boundary Layer on a Vertical Plate at 0.0906 atm Pressure

VII. Discussion of Results

Effect of Reduced Pressure on the Heat Transfer Coefficient

The discussion of the results of the effect of reduced pressure on the heat transfer coefficient will be divided into two parts: (1) comparison of experimental with theoretical results, and (2) factors affecting the results.

Comparison of Experimental and Theoretical Results. The solid line of Figs. 6, 7, 8, and 9 represent the theoretical solution of free-convective heat transfer from a vertical plate for a Prandtl number of 0.70 as determined by solution of the boundary layer equations (Ref 3:315). As can be seen from Figs. 6, 7, and 8 the slope of the experimental line is very nearly the same as the theoretical line. The difference is due to experimental factors, some of which will be discussed later.

Fig. 9 shows that the effect on the Nusselt number is the same regardless of whether the pressure or the dimension is varied to change the Grashof number.

Factors Affecting the Results. Some of the factors which could influence the results are as follows: choice of property reference temperature, error in temperature difference per fringe (ϕ), error in spacing per fringe (Δy), and variation in the plate-chamber temperature difference (θ).

The mean value of the plate and chamber temperatures was used as a reference temperature to evaluate the properties of air in this study. The use of a higher reference temperature to compute the gas properties would have resulted in a lower Grashof number which would shift each point on Figs. 6, 7, 8, and 9 to the left. Similarly, the use of a reference temperature lower than the mean temperature would shift each point to the right. Since each point would be shifted approximately the same amount, the slope of the line through the points in Figs. 6, 7, and 8 would not be greatly affected.

Another factor which could affect the results is the inherent errors in the interferometer, such as end effect and aberration effect (Ref 4:7). However, the interferometer errors would affect each value of the Nusselt number in the same manner and shift each point on Figs. 6, 7, 8, and 9 up or down. Therefore, the slope of the line through the points (m) would not be greatly affected by the interferometer errors.

The factor which caused the greatest scatter in the data points on the graphs was the error in measuring the spacing between fringes near the wall. The spacing between fringes became greater as the pressure was decreased as shown in Figs. 10 through 14. The greater spacing between fringes required more judgement; therefore, a greater possibility of error existed in determining the center of

the fringe in the measuring process. Therefore, an effort was made to decrease the spacing between fringes.

A decrease in spacing between fringes was accomplished by using a blue filter instead of the green filter with the mercury lamp. Fig. 15 shows a comparison of the fringe spacing obtained with the blue and green filters. Figs. 6, 7, and 8 show that data obtained using the blue filter agrees very well with the theoretical equation.

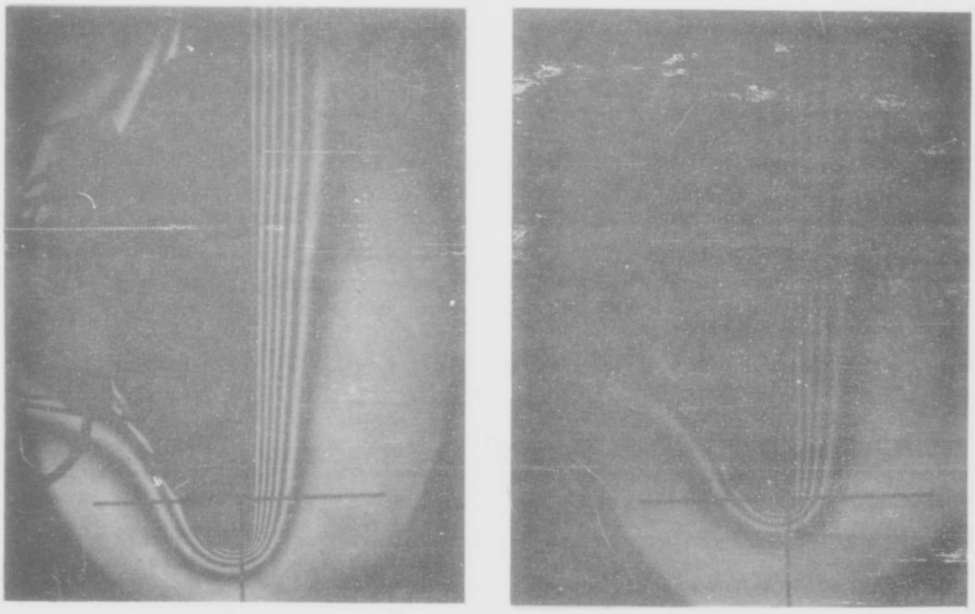

Blue Filter Green Filter

Fig. 15

Interferogram Fringe Spacing

The variation of the plate-chamber temperature (θ) could have had a direct influence on the results. The first set of data (Table I) was obtained using an initial plate-chamber temperature difference (θ) of 101°F. A second set of data (Table II) was obtained using an initial (θ) of 88°F. It was found that the first set of data with the larger θ generally gave a larger value of the Nusselt number than the second set of data for the same value of the product of Prandtl and Grashof numbers. Shine also noticed that the Nusselt number increased with increased θ for a constant value of the product of Prandtl and Grashof numbers, during an interferometer study on free convection (Ref 10:54). Tables I and II show that θ increases as the pressure decreases. The increase in θ with decrease of pressure could explain the reason for the slope of the experimental line to be less than that of the theoretical line in Figs. 6, 7, and 8.

Effect of Reduced Pressure on the Boundary Layer

In the preceeding section the heat transfer coefficient was found to decrease with decreasing pressure. It would follow then that the resistance to heat transfer increases as the pressure is decreased. Figs. 10 through 14 illustrate this, as the boundary layer thickness which offers the resistance to heat flow is seen to increase with decreasing pressure.

The decreasing number of fringes with decreasing pressure, as shown in Figs. 10 through 14, can be explained by considering Eq (9).

$$\Delta T = T_c \left[\frac{\lambda_o \mathcal{E}}{CL\gamma_c - \lambda_o \mathcal{E}} \right] \qquad (9)$$

The temperature difference between fringes increases as density of the air in the chamber (γ_c) is lowered by lowering the chamber pressure. Therefore, the number of fringes in the boundary layer decreases for a given plate-chamber temperature difference.

The temperature boundary layer thickness in Figs. 10 through 14 becomes difficult to define as the pressure is decreased. For example, the difference between the chamber temperature and the temperature of the first fringe in Fig. 10 is 4.20°F. Whereas, in Fig. 14 the difference between the chamber temperature and the temperature of the first fringe is 55.5°F. The partial white fringe around the rear of the plate in Fig. 14 is the result of the plate-chamber temperature difference not being great enough to produce one complete fringe.

VIII. Conclusions

Based on the interferometer study of the effect of reduced pressure on free convection from a vertical plate presented in this report, the following conclusions are drawn:

1. The free-convective heat transfer coefficient is proportional to the 0.47 power of the pressure which is within experimental limits of the theoretical prediction (0.50 power of the pressure).

2. The free convection boundary layer thickness increased as the pressure decreased.

3. The effect on the Nusselt number is the same regardless of whether the pressure or a dimension is varied to change the Grashof number.

4. A blue light source for the interferometer will give more fringes than a conventional green light source, resulting in better accuracy in determining the Nusselt number at air pressures below 0.400 atm.

5. The interferometer can be used with good results for free convection studies at sub-atmospheric pressures.

Bibliography

1. Brown, A. I., and S. M. Marco. Introduction to Heat Transfer (Third Edition). New York: McGraw-Hill, 1958.

2. Eckert, E. R. G., et al. Manufacture of a Zehnder-Mach Interferometer AFTR 5721. Wright-Patterson Air Force Base, Ohio: USAF Air Material Command, 1948.

3. Eckert, E. R. G., and R. M. Drake. Heat and Mass Transfer. New York: McGraw-Hill, 1959.

4. Eckert, E. R. G., and E. E. Soehngen. Studies on Heat Transfer in Laminar Free Convection with the Zehnder-Mach Interferometer AFTR 5747. Wright-Patterson Air Force Base, Ohio: Wright Air Development Center, 1948.

5. Jakob, Max, and G. A. Hawkins. Elements of Heat Transfer and Insulation. New York: John Wiley and Sons, Inc., 1942.

6. Kreith, Frank. Principles of Heat Transfer. Scranton, Pennsylvania: International Textbook Co., 1959.

7. Madden, A. J., et al. "Natural-Convection Heat Transfer at Reduced Pressure." Chemical Engineering Progress, 49:653-660 (December 1953).

8. Physics Staff. Engineering Physics Laboratory Manual (Fourth Edition). Wright-Patterson Air Force Base, Ohio: USAF Institute of Technology, September 1955.

9. Shapiro, Ascher H. The Dynamics and Thermodynamics of Compressible Fluid Flow Volume I. New York: The Ronald Press Co., 1953.

10. Shine, A. J. The Effect of Transverse Vibrations on the Heat-Transfer Rate from a Heated Vertical Plate in Free Convection. Dissertation. Columbus, Ohio: The Ohio State University. 1957.

Appendix A

Data

TABLE I

DATA FROM RUN No. I

P_c atm	T_r °F	T_c °F	θ °F	Station x=2		Station x=3		Station x=4	
				PrGr	Nu	PrGr	Nu	PrGr	Nu
0.975	65	71.0	101.0	4.80×10^5	9.64	1.62×10^6	12.9	3.84×10^6	16.4
0.925	65	71.0	102.0	4.34	9.76	1.46	13.1	3.48	16.2
0.874	65	71.0	103.0	3.90	9.56	1.32	13.1	3.12	16.3
0.799	68	65.4	107.3	3.52	9.50	1.18	12.7	2.82	15.5
0.761	65	67.4	107.8	3.13	9.06	1.06	12.5	2.51	15.4
0.715	68	72.3	108.9	2.61	9.00	8.80×10^5	11.9	2.09	14.7
0.628	66	70.0	111.3	2.08	8.60	7.03	11.7	1.67	14.1
0.590	66	71.0	114.0	1.86	8.25	6.26	11.3	1.49	13.4
0.561	74	74.0	115.0	1.62	7.60	5.46	10.2	1.30	13.3
0.527	75	75.8	117.2	1.42	7.50	4.80	10.3	1.14	13.1
0.497	71	77.0	117.7	1.24	7.41	4.19	9.91	9.95×10^5	12.8
0.470	72	78.0	118.5	1.11	6.90	3.74	9.76	8.88	12.5
0.450	72	79.0	122.3	1.02	7.25	3.44	9.75	8.19	12.2
0.430	67	73.5	121.2	9.84×10^4	6.86	3.31	9.60	7.87	12.3
0.394	68	74.8	123.2	8.17	6.45	2.75	8.95	6.54	11.6
0.367	69	76.0	124.0	7.24	6.55	2.44	9.21	5.79	11.8
0.339	71	77.8	127.2	6.02	6.30	2.02	8.91	4.81	11.2
0.312	71	79.0	128.7	5.07	6.41	1.71	8.80	4.05	11.1
0.284	74	82.0	132.4	3.62	5.42	1.22	7.30	2.90	9.37
0.250	75	84.8	133.2	2.69	5.23	9.04×10^4	7.34	2.15	9.50
0.221	69	80.0	139.7	2.63	5.24	8.85	7.31	2.10	9.43
0.204	69	81.0	140.5	2.26	5.47	7.60	7.40	1.81	9.45
0.1956	70	82.0	139.5	2.06	4.72	7.01	6.51	1.67	8.22
0.1831	72	85.0	139.0	1.75	4.73	5.90	6.60	1.40	8.20
0.1684	72	85.0	139.7	1.48	4.45	4.99	5.87	1.19	7.35
0.1580	74	86.0	140.3	1.30	4.30	4.36	5.60	1.04	6.70
0.0906	70	77.0	149.0	4.62×10^3	3.20	1.55	4.40	3.69×10^4	5.42

TABLE II

DATA FROM RUN No. II

P_c atm	T_r °F	T_c °F	θ °F	Station x=2		Station x=3		Station x=4	
				PrGr	Nu	PrGr	Nu	PrGr	Nu
0.987	67	70.0	88.0	4.50×10^5	10.0	1.51×10^6	13.0	3.61×10^6	16.6
0.954	67	70.2	89.8	4.24	9.16	1.43	12.8	3.40	16.5
0.940	67	70.2	89.9	4.10	9.24	1.39	12.4	3.29	16.6
0.920	69	71.0	90.2	3.94	9.51	1.32	12.7	3.14	16.3
0.894	70	73.0	91.0	3.72	8.46	1.26	12.0	2.98	15.7
0.854	71	74.1	92.4	3.42	9.21	1.15	11.9	2.74	15.7
0.825	71	75.8	93.0	3.14	8.66	1.06	11.7	2.52	14.8
0.788	72	76.1	94.1	2.85	8.50	9.60×10^5	11.8	2.28	14.9
0.757	72	76.3	95.2	2.73	8.10	9.19	11.6	2.18	14.3
0.720	72	76.1	96.1	2.43	8.00	8.19	11.4	1.94	14.8
0.686	73	76.4	99.6	2.24	8.56	7.56	11.3	1.80	14.2
0.658	74	79.1	99.7	1.90	7.46	6.40	10.2	1.52	12.7
0.610	74	79.8	99.2	1.74	7.80	5.81	10.8	1.39	13.4
0.578	73	79.1	101.9	1.58	7.58	5.31	10.7	1.26	13.0
0.540*	73	78.9	102.5	1.39	7.90	4.68	10.2	1.11	12.2
0.502	73	78.8	103.3	1.20	7.40	4.02	9.90	9.55×10^5	12.0
0.468	73	78.5	107.5	1.06	7.01	3.50	9.90	8.46	12.1
0.444	72	78.0	106.0	9.44×10^4	7.03	3.18	9.50	7.55	11.8
0.399	74	80.5	109.2	7.61	6.24	2.56	8.90	6.09	10.8
0.386	75	82.0	112.5	6.31	6.57	2.14	8.90	5.09	10.8
0.298	73	79.0	115.0	4.38	5.68	1.48	7.20	3.51	9.31
0.212	75	82.9	120.7	2.22	4.83	7.46×10^4	6.64	1.77	8.55
0.1129	75	82.0	134.0	6.84×10^3	3.50	2.24	4.65	5.31×10^4	5.74

* Note: Data was obtained using a blue light source at P equal 0.540 and below

Appendix B

Development of Table For Interferogram Temperature Evaluation

Development of $\Delta T = T_c\left[\frac{\lambda_o \epsilon}{CL\gamma_c - \lambda_o \epsilon}\right]$

Soehngen and Eckert developed an expression for the density of a fringe in the boundary layer given by

$$\gamma = \gamma_c\left[1 - \frac{\lambda_o \epsilon}{\gamma_c CL}\right] \qquad \text{(Ref 4:2-3)} \qquad (15)$$

Combining the equation of state for a perfect gas and Eq (15) results in

$$T = \frac{P}{R\gamma} = \frac{P}{R\gamma_c\left[1 - \frac{\lambda_o \epsilon}{\gamma_c CL}\right]} \qquad (16)$$

Using the assumption $P = P_c$ in the boundary layer and the equation of state for a perfect gas, Eq (16) becomes

$$T = T_c\left[\frac{\gamma_c CL}{\gamma_c CL - \lambda_o \epsilon}\right] \qquad (17)$$

The temperature difference between any fringe and the reference temperature is given by

$$\Delta T = T - T_c \qquad (18)$$

Substituting Eq (17) into Eq (18) gives

$$\Delta T = T_c\left[\frac{\gamma_c CL}{\gamma_c CL - \lambda_o \epsilon} - 1\right] \qquad (19)$$

or the desired result:

$$\Delta T = T_c\left[\frac{\lambda_o \epsilon}{CL\gamma_c - \lambda_o \epsilon}\right] \qquad (9)$$

Computer Program for Table III

Fig. 16 shows the digital computer program for the bracketed portion of Eq (9). This program can serve as a guide in the preparation of tables for different model lengths from the 10 inch length used in Table III.

```
 160001000000RS160001000000RS
ENTER SUBRØUTINES, PUSH START
1620 FØRTRAN SUBR.   9/30/61
LØAD DATA
160001000000RS
ENTER SUBRØUTINES, PUSH START
1620 FØRTRAN SUBR.   9/30/61
LØAD DATA160001000000RS
ENTER SØURCE PRØGRAM, PUSH START
ØØ300 C      FØRTRAN TEMPERATURE DIFFERENCE CALCULATIØN
ØØ300        GAMA=.0750
ØØ336        CØNST=3.03E-3
ØØ372        BDAØ=1.791645E-6
ØØ408        DØ9 I=1,35
ØØ420        EPS=1.0
ØØ456        GAMA=GAMA-.001
ØØ504        PRINT 6,GAMA
ØØ528        DØ7 J=1,30
ØØ540        B=(BDAØ*EPS)/(CØNST*GAMA-BDAØ*EPS)
ØØ696        PRINT 8,B
ØØ720        EPS=EPS+1.0
ØØ768 7      CØNTINUE
ØØ804 9      CØNTINUE
ØØ840 6      FØRMAT(F9.4)
ØØ862 8      FØRMAT(F10.6)
ØØ884        END
```

Fig. 16

Computer Program for Table III

Table III*

Table of $\left[\frac{\lambda_o \varepsilon}{CL\gamma_c - \lambda_o \varepsilon}\right]$ for Interferogram

Temperature Evaluation

The temperature T represented by fringe ε is given by

$$T - T_c = T_c \left[\frac{\lambda_o \varepsilon}{CL\gamma_c - \lambda_o \varepsilon}\right]$$

Symbols

λ_o	5461 $\mathring{A}$
ε	Fringe number
L	Length of plate, 10 inches
C	Constant, 0.003636 ft^3/lb_m
γ_c	Density of reference air, ft^3/lb_m
T_c	Temperature of reference air, ^oF

*The remainder of Table III, for values of γ_c from 0.0710 to 0.000, is located in the AFIT Mechanical Engineering Department files.

Table III

$$\left[\frac{\lambda_o \varepsilon}{CL\gamma_c - \lambda_o \varepsilon}\right]$$

ε	$\gamma_c = .0740$	$\gamma_c = .0730$	$\gamma_c = .0720$
1	.008054	.008166	.008280
2	.016240	.016466	.016699
3	.024560	.024905	.025259
4	.033017	.033485	.033965
5	.041615	.042209	.042820
6	.050357	.051082	.051829
7	.059247	.060108	.060994
8	.068290	.070320	.071381
9	.077487	.078632	.079811
10	.086845	.088139	.089437
11	.096366	.097815	.099309
12	.106056	.107665	.109324
13	.115918	.117693	.119523
14	.125958	.127904	.129912
15	.136180	.138304	.140495
16	.146590	.148897	.151278
17	.157192	.159689	.162267
18	.167992	.170686	.173468
19	.178996	.181894	.184887
20	.190208	.193318	.196530
21	.201636	.204965	.208405
22	.213286	.216841	.220517
23	.225164	.228955	.232875
24	.237277	.241311	.245486
25	.249631	.253919	.258357
26	.262235	.266786	.271497
27	.275095	.279919	.284914
28	.288221	.293327	.298618
29	.301619	.307020	.312617
30	.315299	.321005	.326921

Vita

Captain Richard C. Walker was born [redacted] in [redacted]. After completing his work in 1950 at [redacted], he entered South Dakota State College, Brookings, South Dakota. He was graduated in 1954 with a degree in Agricultural Engineering. He immediately entered the Air Force where he has served as an F-89 interceptor pilot at Portland, Oregon, and Fairbanks, Alaska. He was assigned as a T-33 flight instructor prior to his entry to the Institute of Technology in 1960.

Permanent address: [redacted]

This thesis was typed by Mrs. Carol Walker.

UNCLASSIFIED